Estimation of Sea State Parameters from Onboard Real Ship Motions Using an Adaptive Kalman Filter

Ryane Bourkaib
Delft University of Technology,
Department of Ship Hydrodynamics,
Delft, The Netherlands.
Email: r.b.bourkaib@tudleft.nl

Manon Kok
Delft University of Technology,
Delft Center for Systems and Control,
Delft, The Netherlands.
Email: M.Kok-1@tudelft.nl

Harleigh Seyffert
Delft University of Technology,
Department of Ship Hydrodynamics,
Delft, The Netherlands.
Email: H.C.Seyffert@tudelft.nl

***Abstract*—Accurately estimating sea state parameters is crucial for ship safety and efficiency. The objective of this paper is to study the applicability of the Adaptive Kalman filter (AKF) to estimate sea state parameters—significant wave height, peak period, and relative mean wave direction—using onboard ship motion measurements. The main idea is to assess the performance of this method under real-world conditions including varying ship forward speed and heading and noisy measurements. In this study, data recorded from onboard the United States Coast Guard Cutter (USCGC) STRATTON is considered for testing the method. The method's performance is evaluated by comparing the estimated sea state parameters to those obtained from the Copernicus hindcast model. The obtained results show the AKF's capacity to estimate sea state parameters under real-world conditions, such as variable forward speeds and potential sensor and model inaccuracies.**

***Keywords* —Sea state estimation, Directional wave spectrum estimation, Adaptive Kalman filter, Ship motions, In-service data, Copernicus model, Time domain estimation.**

I. Introduction

Ship accidents can have serious consequences, including loss of life and damage to the environment. To improve operational safety, ships can rely on decision support systems that use real-time data to detect dangerous conditions early on [1]. For this type of system, the directional wave spectrum needs to be estimated and updated in real-time operation [1]. One of the most cost-effective methods for obtaining sea state parameters is by considering a ship as a wave buoy itself, via the ship as a wave buoy (SAWB) analogy [2]. This method combines ship motion measurements with a transfer function that defines the relationship between wave input and the ship's motion response, allowing for real-time sea state estimation. Most studies on SAWB have been performed in the frequency domain (e.g., [3]–[7]). However, only a few studies have been conducted in the time domain (e.g., [8]–[12]), despite the potential for real-time estimations. For more details, an overview of the existing methods in both the frequency and time domains is provided in [2], [13], [14].

A. Objective

In this study, we focus on a time-domain method—specifically, the Kalman Filter (KF)—because it has shown promising results for real-time sea state estimation, as demonstrated in different studies (e.g., [8], [10], [12]). This method is fast and can handle potential inaccuracies in both measurements and model definitions. Additionally, it is easy to implement [14]. To the authors' best knowledge, this method has only been tested for restrictive assumptions such as zero or low forward speed and with simulated or controlled ship motion data.

To address those gaps, the present authors introduced an Adaptive Kalman Filter (AKF) method in [15] to estimate both unidirectional and multi-directional waves from measured ship motion responses while incorporating the effects of varying forward speed and unknown measurement noise (note that the paper was under review at time of submission). The proposed method was tested in [15] with simulated motion responses and its performance compared well with a baseline frequency domain SAWB method [2]. In this work, we further evaluate the method's performance using ship motion measurements recorded onboard an in-service vessel. The main objective here is to further assess and validate the method's effectiveness under real-world conditions, such as ship forward speed and heading variation, as well as potential sensor and model inaccuracies. Since the ground truth of the sea state cannot be directly measured during operations, we compare our estimated sea state parameters with the Copernicus hindcast model.

B. Composition of the paper

The paper is organized as follows. In Section II the methodology applied is discussed after providing a brief review of the theoretical background and the fundamental equations used. In Section III the case study is described. In Section IV, the obtained results are discussed. Section V is dedicated to the conclusion.

II. Methodology

In this work, we use the AKF to estimate the complex wave components—specifically, the real and imaginary parts of the directional wave spectrum—from ship motion measurements. We then use these estimates to compute the sea state parameters, including significant wave height, peak period, and relative mean wave direction. To achieve this, we first in Section II-A define a model that describes the relationship between ship motion measurements and the incident wave field

OCEANS 2025 Brest | 979-8-3315-3747-0/25/$31.00 ©2025 IEEE | DOI: 10.1109/OCEANS58557.2025.11104745

979-8-3315-3747-0/25/$31.00 ©2025 IEEE

which will be used as a measurement model of the AKF. Subsequently, we define the state space model for the AKF and detail its implementation in Sections II-B and II-C. Finally, we explain how the estimates are used to compute the sea state parameters in Section II-D.

A. Relationship between ship motion and waves

A ship's response to incident waves can be characterized by transfer functions that describe how a ship interacts with waves. In this context, the ship is considered as a wave buoy, which means that the measured responses contain information about the exciting waves. In particular, the ship response y at time t in any degree of freedom l—such as surge, heave, pitch, or roll—can be modeled as:

$$y_l(t) = \sum_{i=1}^{N}\sum_{j=1}^{M}\{\text{RAO}_{lij}\cos(\omega_i t + \varphi_{lij})x_{1,ij} + \text{RAO}_{lij}\sin(\omega_i t + \varphi_{lij})x_{2,ij}\}, \tag{1}$$

where:

- N is the total number of absolute wave frequencies.
- M is the total number of wave directions.
- ω_i is the i-th absolute wave frequency.
- RAO_{lij} and φ_{lij} are the amplitude and phase of the transfer function of the l-th degree of freedom of the ship motion for the i-th frequency and j-th wave direction, respectively.
- $x_{1,ij}$ and $x_{2,ij}$ represent the real and imaginary components of the complex wave for the i-th frequency and j-th direction, respectively.

It is worth noting that Eq.(1) assumes that the ship has zero forward speed, as it uses the absolute wave frequencies ω. In practice, however, a ship operates with a non-zero forward speed, so in this case, the transfer function in Eq.(1) is actually a function of the ship's forward speed. Therefore, a transformation from absolute frequency to encounter frequency must be applied to account for the Doppler shift effect, as outlined by [16]. This transformation can be expressed as follows:

$$\omega_\text{e} = \omega - \omega^2\psi, \quad \text{with } \psi = \frac{U}{g}\cos(\beta), \tag{2}$$

where:

- ω_e is the encounter wave frequency.
- U is the ship's forward speed.
- β is the relative wave direction with 180° corresponding to head seas,
- g is the acceleration due to gravity.

Therefore, Eq.(1) can be refined to include the effects of the ship's forward speed, as follows:

$$y_l(t) = \sum_{i=1}^{N}\sum_{j=1}^{M}(\text{RAO}_{lij}(U)\cos(\omega_{\text{e},i}t + \varphi_{lij}(U))x_{1,ij} + \text{RAO}_{lij}(U)\sin(\omega_{\text{e},i}t + \varphi_{lij}(U))x_{2,ij}), \tag{3}$$

B. State space model

To implement the AKF for complex wave component estimation, we first need to establish a state space model which includes a process model and a measurement model. Note that this filter can be applied only for linear waves and responses and its accuracy may decrease when the nonlinear effects become significant. The process model describes the evolution of the complex wave components over time, and can be defined as:

$$x_{k+1} = \phi_k x_k + w_k, \quad \text{with } w_k \sim \mathcal{N}(0, Q), \tag{4}$$

where:

- $x_k = [x_{1,ij}\cdots x_{1,NM}, x_{2,ij}\cdots x_{2,NM}]^T$ represents the state vector at time instant k of the complex wave components with dimension $2NM$.
- x_{k+1} is the state vector at the next time instant.
- ϕ is the transition matrix with dimension $2NM \times 2NM$. Since the sea state is assumed to be stationary within a time window Δt, ϕ is an identity matrix.
- w_k is the process Gaussian noise vector with dimension $2NM$.
- $\mathcal{N}(0, Q)$ is a normal distribution with zero mean and a process covariance error Q; the dimension of Q is $2NM \times 2NM$.

The discrete measurement model for the ship motion responses can be determined using Eq.(3), as follows:

$$y_k = H_k x_k + v_k, \quad \text{with } v_k \sim \mathcal{N}(0, R_k), \tag{5}$$

where:

$$H_k = \begin{bmatrix} H_{\text{C},k} & H_{\text{S},k} \end{bmatrix}, \tag{6}$$

with,

$$H_{\text{C},k} = \begin{bmatrix} C_{111} & \cdots & C_{1ij} & \cdots & C_{1NM} \\ \vdots & \ddots & \vdots & \ddots & \ddots \\ C_{L11} & \cdots & C_{lij} & \cdots & C_{LNM} \end{bmatrix},$$

$$H_{\text{S},k} = \begin{bmatrix} S_{111} & \cdots & S_{1ij} & \cdots & S_{1NM} \\ \vdots & \ddots & \vdots & \ddots & \ddots \\ S_{L11} & \cdots & S_{lij} & \cdots & S_{LNM} \end{bmatrix},$$

$$C_{lij} = \text{RAO}_{lij}(U)\cos(\omega_{\text{e},i}k\Delta t + \varphi_{lij}(U)),$$

$$S_{lij} = \text{RAO}_{lij}(U)\sin(\omega_{\text{e},i}k\Delta t + \varphi_{lij}(U)),$$

where:

- H_K is the output matrix at time instant k with dimension $L \times 2NM$.

- v_K is the measurement Gaussian noise vector with dimension L.
- $\mathcal{N}(0, R_K)$ is a normal distribution with zero mean and a measurement covariance error R_K. The dimension of R_k is $L \times L$.
- x_k is the state vector with dimension $2NM$.
- L is the number of ship responses used in the AKF.
- k is the number of the time step.
- Δt is the time between sampling instances.

C. AKF implementation

Now that we have determined the state space model, we implement the AKF to estimate the state vector (the complex wave components). This implementation involves two main steps: prediction and correction.

1) Prediction step: In this step, the current state $\hat{x}_k^-$ and its covariance error P_k^- are predicted as follows:

$$\hat{x}_k^- = \hat{x}_{k-1}^+, \tag{7a}$$

$$P_k^- = P_{k-1}^+ + Q. \tag{7b}$$

The state covariance matrix P_k^- is predicted based on its previous value P_{k-1}^+ and the covariance of the process model Q. Note that instead of using a uniform Q for all states, we assign low Q values to high wave frequencies (where the ship response is weak) to deal with the overestimation problem (as seen by, e.g., [17]). This problem arises because the amplitudes of the ship motion transfer functions approach zero at higher frequencies, which when used in the inverse sea state estimation can amplify the sensor noise in the measurements. The threshold for "high wave frequencies" is determined by identifying the frequency range at which the vessel transfer function amplitude becomes negligible.

2) Correction step: In this step, the updated state $\hat{x}_k^+$ and its covariance error P_k^+ are calculated as follows:

$$e_k = y_k - H_k \hat{x}_k^- \tag{8a}$$

$$R_k = \alpha R_{k-1} + (1-\alpha)(e_k e_k^T - H_k P_k^- H_k^T) \tag{8b}$$

$$S_k = H_k P_k^- H_k^T + R_k \tag{8c}$$

$$K_k = P_k^- H_k^T S_k^{-1} \tag{8d}$$

$$\hat{x}_k^+ = \hat{x}_k^- + K_k e_k \tag{8e}$$

$$P_k^+ = (I - K_k H_k) P_k^- \tag{8f}$$

The Kalman gain K_k is calculated using the predicted state covariance P_k^- and the measurement covariance error R_k, as shown in Eq.(8d). Note that R_k is adaptively estimated based on a smoothing factor $0 < \alpha < 1$, which determines the weight given to the previous estimate of R_k, as detailed in Eq.(8b) [18]. We use an adaptive R_k instead of a constant value because the noise covariance is unknown and may vary with changes in the ship's forward speed. The state vector is updated based on its predicted values, the Kalman gain K_k, and the measurement prediction error e_k, as shown in Eq.(8e). The state covariance matrix P_k^+ is then updated based on its predicted value P_k^- and K_k, as shown in Eq.(8f). To conclude, the AKF recursively estimates the state vector using ship motion measurements, helping it manage noisy or incomplete data.

D. Sea state calculation

After we estimate the state vectors $\hat{x}_{1\ldots k}^+$ from ship motion measurements using the AKF, we use them to calculate the absolute directional wave spectrum $S_k(\omega_i, \beta_j)$ as follows:

$$S_k(\omega_i, \beta_j) = \frac{(\hat{x}_{1,ijk}^+)^2 + (\hat{x}_{2,ijk}^+)^2}{2\Delta\omega_i \Delta\beta_j}, \tag{9}$$

where $\hat{x}_{1,ijk}^{+2}$ and $\hat{x}_{2,ijk}^{+2}$ are the estimated real and imaginary complex wave components, respectively, of the i-th and the j-th absolute frequency and relative wave direction at time instant k. Note that since the wave energy is conserved between the encounter and absolute domains, the state vectors $\hat{x}_{1\ldots k}^+$ can be directly used to compute the absolute directional spectrum $S_k(\omega_i, \beta_j)$.

From $S_k(\omega_i, \beta_j)$, we can compute sea state parameters including significant wave height H_{sk}, peak period T_{pk} and relative mean wave direction $\bar{\beta}_k$ as follows:

$$\bar{\beta}_k = \arctan\left(\frac{d_k}{c_k}\right), \tag{10}$$

where:

$$c_k = \int_{-\pi}^{\pi}\int_0^{\infty} S_k(\omega, \beta)\cos(\beta)\, d\omega\, d\beta, \tag{11}$$

$$d_k = \int_{-\pi}^{\pi}\int_0^{\infty} S_k(\omega, \beta)\sin(\beta)\, d\omega\, d\beta. \tag{12}$$

$$H_{sk} = 4\sqrt{M_{0k}} \quad \text{with} \quad M_{0k} = \int S_k(\omega) d\omega, \tag{13}$$

where M_{0k} represents the zeroth spectral moment of the estimated wave energy spectrum at time instant k and $S_k(\omega)$ is the frequency spectrum obtained by summing $S_k(\omega, \beta)$ over β.

$$T_{pk} = \frac{2\pi}{\omega_{pk}}, \quad \text{with} \quad \omega_{pk} = \text{argmax}(S_k(\omega)), \tag{14}$$

where ω_{pk} is the angular frequency corresponding to the maximum amplitude in the estimated wave spectrum.

The calculated sea state parameters (H_{sk}, T_{pk} and $\bar{\beta}_k$) are compared with Copernicus hindcast data to assess the effectiveness of the AKF. The AKF can also estimate the wave elevation using the estimated complex wave components, but since there is no Copernicus comparison, these results are not shown. Note that the ground truth is unknown and the Copernicus hindcast data is also an estimate.

III. Case ship and in-service data

The AKF technique was tested using simulated motion responses for both unidirectional and multi-directional waves by the same authors in [15]. In the present study, the AKF is tested using measurement data recorded onboard an in-service ship. The case ship is the USCGC STRATTON with main particulars specified in Tab. I.

TABLE I
MAIN PARTICULARS OF THE USCGC STRATTON [19]

Main Particular	Value
Length overall	127.29 m
Length between perpendiculars	118.87 m
Beam, waterline	14.90 m
Beam, maximum	16.46 m
Design draft	4.39 m
Block coefficient	0.492
Displacement (fully appended)	4571 tonnes

The ship was installed with a motion sensor mounted close to its centreline. This sensor provides ship motion measurements in six degrees of freedom (DOF) including surge, sway, heave, roll, pitch, and yaw. For the sea state estimation, we used only sway, heave, roll, and pitch. The ship was also installed with a GPS sensor, which provides continuous information on the ship's forward speed. Note that the transfer functions should be based on the vessel's speed through water (STW), not the speed-over-ground (SOG) provided by GPS data [6]. Using GPS data directly can lead to errors in the transfer function, especially in areas where currents are significant. Since the ship is not equipped with a sensor to measure STW, we use the SOG and consider the error between STW and SOG as a measurement model error in the AKF. To ensure data quality, we implemented filtering procedures such as a bandpass filter with low cut-off of 0.6rad/s and high cut-off of 20rad/s, and we synchronized the data at the same sample frequency ($10Hz$). The corresponding transfer functions of this vessel at different forward speeds were provided by the Maritime Research Institute Netherlands (MARIN), which has carried out extensive monitoring campaigns for this vessel (see, e.g., [19], [20]).

During the voyage, measurements for one day were collected. This data was divided into segments with a time duration of 1000s. For each segment, we performed the Fourier transform to identify the wave frequency ranges based on the spectral energy. By analyzing the resulting spectrum, we can see which frequency bands have significant energy peaks. Only frequencies between 0.1rad/s and 2rad/s were considered as no significant wave-induced motions occur outside this interval. Then, for each motion segment, the state vector has been estimated using the AKF.

In the implementation of this filter, specifically, the output matrix described by Eq.(6), the wave frequency domain was discretized into 38 bins over the interval $\omega = [0.1, 2]$rad/s with $\Delta\omega = 0.05$rad/s. To account for the vessel's forward speed, we used the encounter wave frequency ω_{e} instead of the wave frequency ω, as shown in Eq.(2). Additionally, the relative wave direction was discretized into 7 bins over the interval $\beta = [90^\circ, 270^\circ]$. We chose this interval based on prior knowledge—Copernicus hindcast data shows that the actual wave directions typically range from 127° to 250°. This information helps reduce the state dimension required for estimation. Note that the state estimation accuracy heavily depends on the chosen discretization of the encounter wave frequency and relative wave direction, as the size of the state depends on the number of discretization bins. In other words, using small $\Delta\omega$ results in a larger number of states to be estimated, leading to a decrease in the filter's accuracy due to the added complexity. Therefore, it is important to find an optimal number of frequencies to ensure reliable state estimation. The relative wave direction is defined such that $\beta = 180^\circ$ corresponds to head seas and $\beta = 0^\circ$ corresponds to following seas, with positive values indicating waves approaching from one side (typically the starboard side) and negative values indicating waves from the port side [6].

The transfer functions used in the AKF, specifically in the output matrix H_k were updated based on significant changes in ship forward speed. Large variations in ship speed mean the current transfer functions (which model the ship's dynamic response) may no longer be valid. The "significant change" in forward speed is determined by comparing the differences between transfer functions calculated for six speeds ranging from 2.5m/s to 14.4m/s and the current forward speed recorded from the GPS. It then selects the transfer function that most closely matches the current speed. Note that for small fluctuations of speed, the average speed is used to smooth out minor variations, thereby preventing unnecessary updates to the transfer functions. The parameters for the AKF are set as follows: the initial state vector $\hat{x}_0^+$ is initialized to zero since no prior information is available. The diagonal values of the process covariance matrix Q are set to 0.1, with reduced values of 0.0015 for high frequencies ($\omega > 1.2$rad/s). Similarly, the diagonal values of the initial state covariance matrix P_0 are set to 10, with lower values of 0.1 at high frequencies. Finally, the initial measurement covariance is defined with diagonal values of 10^{-2} for translational and rotational motions.

IV. RESULTS AND DISCUSSION

The sea state parameters were estimated over time using the AKF, as demonstrated in Section II-D. The average values computed over the last 50 seconds—specifically, significant wave height $H_{s,\text{AKF}}$, peak period $T_{p,\text{AKF}}$, and relative wave direction $\bar{\beta}_{\text{AKF}}$— are presented in Fig. 1, Fig. 2, and Fig. 3, respectively. In each figure, these estimates are directly compared with those obtained from the Copernicus model ($H_{s,\text{CHD}}$, $T_{p,\text{CHD}}$, $\bar{\beta}_{\text{CHD}}$). Note that for each segment, an average over the last 50 seconds is applied to smooth out short-term fluctuations.

From Fig. 1 and Fig. 2, we notice that there is a reasonable agreement between the results of the AKF and those obtained from the Copernicus model for most segments of data. However, there are segments where the significant wave height and peak period are overestimated or underestimated. While a single explanation for these discrepancies is unclear, several factors may contribute. First, this can be explained by the mismatch between the measurement model and the measurement motion data, possibly due to significant non-linearities that the measurement model does not capture. Specifically, the AKF assumes linear wave and response behavior, and its accuracy may be reduced when non-linear

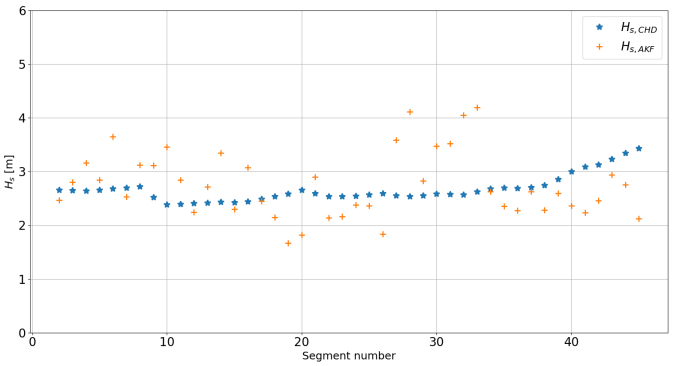

Fig. 1. The estimated significant wave height obtained from the AKF (Eq.(13)) and the corresponding estimates obtained by the Copernicus Hindcast model (CHD).

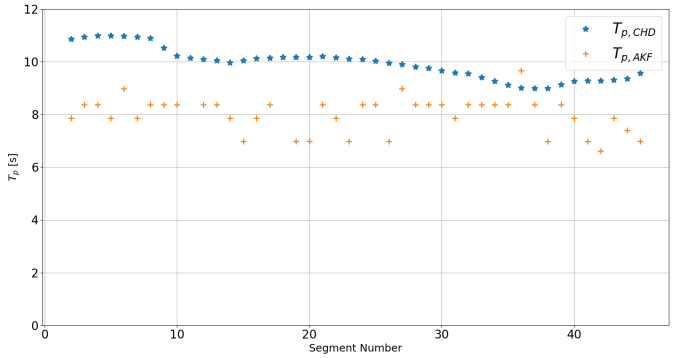

Fig. 2. The estimated peak period obtained from the AKF (Eq.(14)) and the corresponding estimates obtained by the Copernicus Hindcast model (CHD).

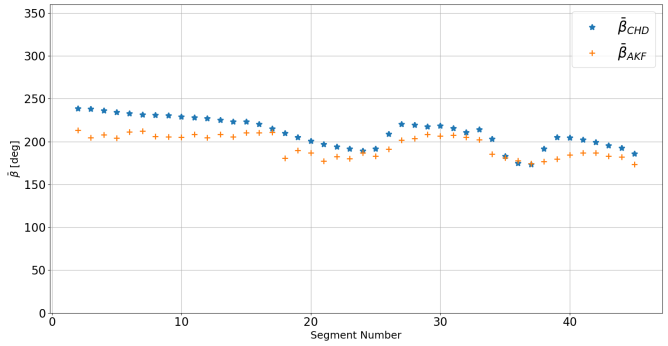

Fig. 3. The estimated relative wave direction from the AKF (Eq.(10)) and the corresponding estimates obtained by the Copernicus Hindcast model (CHD).

effects become significant. Additionally, uncertainties in the transfer functions—determined using SOG data rather than STW speed—may also affect the accuracy of the estimates, as precise transfer functions are critical for reliable results, as demonstrated by [6].

As shown in Fig. 3, the estimated relative wave direction from the AKF and the corresponding estimates from the Copernicus Hindcast model are closely aligned for most segments of the dataset, and they follow a similar trend. However, in some segments, there is an underestimation of the relative

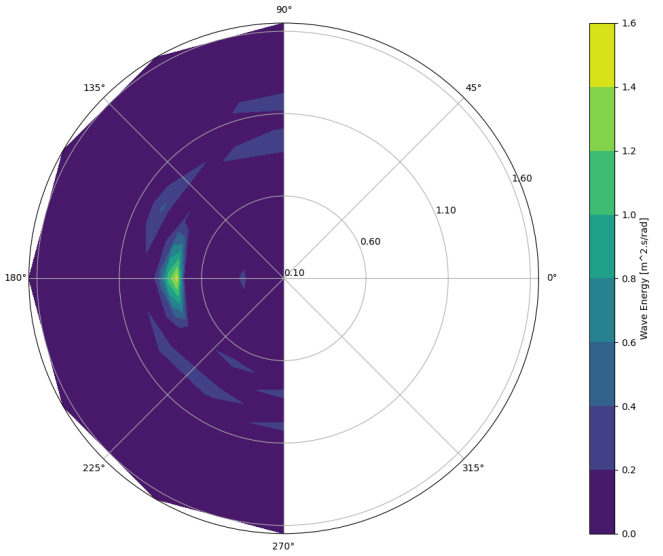

Fig. 4. The estimated directional wave spectrum from the AKF for a segment of $H_{s,\text{CHD}} = 2.70$m, $T_{p,\text{CHD}} = 9.08$s, $\bar{\beta}_{\text{CHD}} = 180.03°$.

wave direction (around an average error of 13°).

The polar plot of the estimated directional wave spectrum of segment 35 (Fig. 1) is shown in Fig. 4. The presented segment is of quite a general nature, including some changes in forward speed (ranging approximately between 13.6 and 19.44 knots with an average of 8.93 knots) and heading (ranging approximately between 284° and 300° with an average of 293°). This segment, as determined from the Copernicus model, has a significant wave height of 2.70m, a peak period of 9.08s, and a relative mean wave direction of 180.03°. In this figure, we observe that most of the wave energy is concentrated around head waves with a relative wave direction of 179.28°, which is close to the one obtained from the Copernicus model. Based on the equations described in Section II-D, the estimated values H_s and T_P from the AKF method are 2.24m and 8.38s, respectively. These values are close to the Copernicus values with an error of approximately 0.5m in H_s and an error of about 0.5s in T_p.

Fig. 5, Fig. 6, and Fig. 7 present comparative plots, illustrating the ratios of the sea state from the AKF and Copernicus hindcast data for the significant wave height, peak period, and relative wave direction, respectively. The ratios are calculated as follows:

$$\text{ratio} = \frac{\text{ESS}_{\text{AKF}}}{\text{ESS}_{\text{CHD}}}, \tag{15}$$

where, ESS_{AKF} and ESS_{CHD} represent the estimated sea state parameter from the AKF and Copernicus hindcast model, respectively. Note that a ratio equal to one indicates a perfect match between the parameter estimated from the AKF and the Copernicus hindcast data. According to Fig. 5, Fig. 6, and Fig. 7, we observe that the ratio is close to 1 for most segments (never exceeds 1.5 or drops below 0.73, except for three segments in Fig. 5). This indicates that the AKF estimates of significant wave height, peak period, and relative

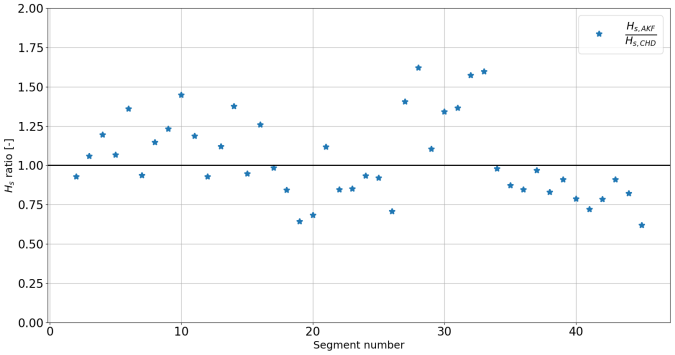

Fig. 5. The ratio between the significant wave height from the AKF and the Copernicus Hindcast model (CHD) calculated using Eq.15.

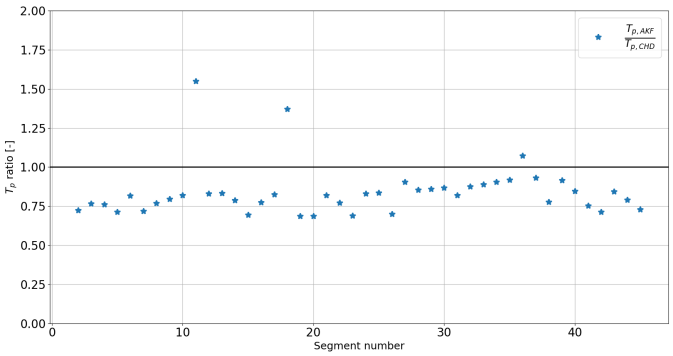

Fig. 6. The ratio between the peak period from the AKF and the Copernicus Hindcast model (CHD) calculated using Eq.15.

wave direction are reasonably accurate and remain close to the Copernicus hindcast. To quantify the deviations, we compute the average of the relative deviation div_{para} for each parameter as follows:

$$\text{div}_{\text{para}} = \frac{\text{ESS}_{\text{AKF}} - \text{ESS}_{\text{CHD}}}{\text{ESS}_{\text{CHD}}}, \tag{16}$$

which yields $\text{div}_{H_s} = 0.040, \text{div}_{T_p} = -0.16, \text{div}_{\bar{\beta}} = -0.082$. These values indicate that the relative deviations of the AKF estimates from the Copernicus hindcast data are within acceptable error bounds. In particular, the deviation in T_p is larger compared to the deviation in H_s and $\bar{\beta}$. One of the reasons for this discrepancy is uncertainties in the transfer functions. In our case, these functions were determined using SOG data instead of STW, and such imprecision can significantly affect the accuracy of the estimates, as demonstrated by [6].

V. CONCLUSION

This study evaluated the applicability of the AKF for estimating sea state parameters including significant wave height, peak period, and relative wave direction from real ship motion data recorded onboard an in-service vessel. The results demonstrated reasonable agreement between the estimates obtained from the AKF and the Copernicus hindcast model, confirming the potential of its application under realistic operational conditions such as small varying forward speeds, headings, and noisy measurements. Additionally, the overestimation issue at

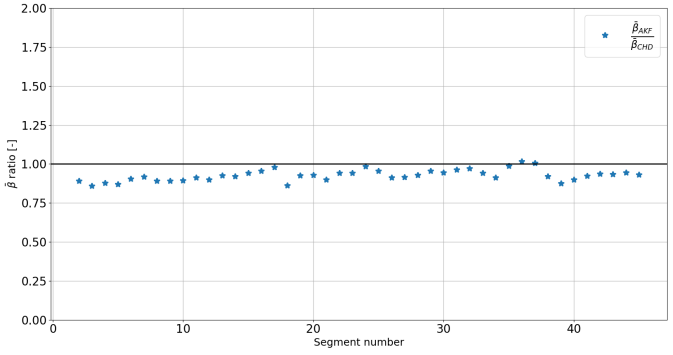

Fig. 7. The ratio between the relative wave direction from the AKF and the Copernicus Hindcast model (CHD) calculated using Eq.(15).

high frequencies due to low motion responses and amplified noise has been addressed by assigning low values to the process and state covariance matrices. The observed discrepancy in some segments can be explained by several factors including the non-linearities that may not be captured by the linear assumptions in the AKF and uncertainties in transfer functions derived using SOG rather than STW. Another point to consider is that in this study, we assume that we have prior knowledge of the location of the relative wave direction to reduce its interval. If all possible wave directions were considered, the estimation accuracy would decrease as the number of states to estimate increased. A potential plan for future work to improve the overall accuracy is to integrate other sensor sources including radar data which can provide an accurate range of wave direction.

As another direction for future work, the AKF method should be further evaluated using additional onboard ship motion data to investigate its performance under various sea conditions, noticing that in the present study, the method was only evaluated for head and quartering seas. Additionally, further studies should incorporate STW measurement to improve the precision of transfer functions, as was demonstrated by [6]. Another point to focus on is non-linearities in the vessel's response that may be present, so developing a method that explicitly accounts for these nonlinearities is required. This could be achieved by replacing the linear transfer function with a nonlinear unified state space model proposed by [21].

ACKNOWLEDGMENT

This publication is part of the project "FUSION: Smart Sensing for Informed Maintenance & Optimized Naval Design" (project number KICH1.VE02.20.010) of the research program "Maritime High-tech for Safer Seas" which is (partly) financed by the Dutch Research Council (NWO). The authors also gratefully acknowledge support from the FReady (Fleet Ready combination of physical virtual hull structure monitoring) JIP.

REFERENCES

[1] E. Boulougouris, J. Cichowicz, A. Jasionowski, and D. Konovessis, "Improvement of ship stability and safety in damaged condition through

operational measures: Challenges and opportunities," *Ocean Engineering*, 2016.
[2] U. D. Nielsen, "A concise account of techniques available for shipboard sea state estimation," *Ocean Engineering*, 2017.
[3] T. Iseki and D. Terada, "Bayesian estimation of directional wave spectra for ship guidance system," *International Journal of Offshore and Polar Engineering*, 2002.
[4] N. Montazeri, U. Nielsen, and J. Jensen, "Selection of the optimum combination of responses for wave buoy analogy - an approach based on local sensitivity analysis," in *Proceedings of the 13th International Symposium on PRActical Design of Ships and Other Floating Structures (PRADS 2016)*. Technical University of Denmark, 2016.
[5] A. H. Brodtkorb and U. D. Nielsen, "Automatic sea state estimation with online trust measure based on ship response measurements," *Control Engineering Practice*, 2023.
[6] U. D. Nielsen and J. Dietz, "Ocean wave spectrum estimation using measured vessel motions from an in-service container ship," *Marine Structures*, 2020.
[7] U. D. Nielsen, H. Bingham, A. Brodtkorb, T. Iseki, J. Jensen, M. Mittendorf, R. Mounet, Y. Shao, G. Storhaug, A. Sørensen, and T. Takami, "Estimating waves via measured ship responses," *Scientific Reports*, 2023.
[8] R. Pascoal and C. Guedes Soares, "Kalman filtering of vessel motions for ocean wave directional spectrum estimation," *Ocean Engineering*, 2009.
[9] D. J. Belleter, R. Galeazzi, and T. I. Fossen, "Experimental verification of a global exponential stable nonlinear wave encounter frequency estimator," *Ocean Engineering*, 2015.
[10] H. Kim, J. Park, C. Jin, M. Kim, and D. Lee, "Real-time inverse estimation of multi-directional random waves from vessel-motion sensors using kalman filter," *Ocean Engineering*, 2023.
[11] Y. Komoriyama, K. Iijima, A. Tatsumi, and M. Fujikubo, "Identification of wave profiles encountered by a ship with no forward speed using kalman filter technique and validation by tank tests - long-crested irregular wave case -," *Ocean Engineering*, 2023.
[12] Y. Komoriyama, K. Iijima, H. Houtani, A. Tatsumi, and M. Fujikubo, "Kalman filter technique for estimating encountered wave profiles and unmeasured ship responses using measurement data in short-crested irregular waves," *Applied Ocean Research*, 2025.
[13] H. Majidian, L. Wang, and H. Enshaei, "Part. A: a review of the real-time sea-state estimation, using wave buoy analogy," *Ocean Engineering*, 2022.
[14] ——, "Part. B: a review of the real-time sea-state estimation, using wave buoy analogy; a decuple benchmark and future outlook," *Ocean Engineering*, 2022.
[15] R. Bourkaib, M. Kok, and H. Seyffert, "Unidirectional and multi-directional wave estimation from ship motions using an adaptive kalman filter with the inclusion of varying forward speed," *under review: Probabilistic Engineering Mechanics*, 2025. [Online]. Available: https://surfdrive.surf.nl/files/index.php/s/TFkZFsuxJf7dGx7
[16] U. D. Nielsen, "Transformation of a wave energy spectrum from encounter to absolute domain when observing from an advancing ship," *Applied Ocean Research*, 2017.
[17] R. Pascoal, L. Perera, and C. Guedes Soares, "Estimation of directional sea spectra from ship motions in sea trials," *Ocean Engineering*, 2017.
[18] S. Akhlaghi, N. Zhou, and Z. Huang, "Adaptive adjustment of noise covariance in kalman filter for dynamic state estimation," in *IEEE Power & Energy Society General Meeting*, 2017.
[19] K. Stambaugh, I. Drummen, R. Hageman, and I. Thompson, "Hull structural monitoring of USCG cutters to support long term maintenance decisions," *ASNE-TSS, Wash. DC, USA*, June 2019.
[20] I. Drummen, L. Rogers, A. Benhamou, R. Hageman, and K. Stambaugh, "Hull structure monitoring of a new class of US coast guard cutters," *ASNE- Technology, Systems & Ships, Wash. DC, USA*, June 2019.
[21] R. Sandeepkumar, S. Rajendran, R. Mohan, and A. Pascoal, "A unified ship manoeuvring model with a nonlinear model predictive controller for path following in regular waves," *Ocean Engineering*, 2022.